

Enhancing the Power Quality Of Distributed Power System Networks

G. Chandu¹, M. Sekhar²

¹ M.Tech Scholar Dept. of Electrical & Electronics Engineering, CRIT, Anantapur.

² Assistant Professor Dept. of Electrical & Electronics Engineering, CRIT, Anantapur.

Abstract:

This paper introduces a novel Power Quality Index (PQI) directly linked to the generation of distortion power from nonlinear harmonic loads, aiming to assess their harmonic pollution ranking within a distribution power system. The Electric Load Composition Rate (LCR) and Total Harmonic Distortion (THD) are estimated using the Reduced Multivariate Polynomial (RMP) model with a one-shot training property. Subsequently, the distortion power ranking for each nonlinear load, indicative of its adverse impact on the entire system, is determined. This ranking quantifies the negative effect each nonlinear load has on the point of common coupling concerning distortion power. The effectiveness and validity of the proposed PQI are confirmed through simulation results conducted via harmonic current injection model-based time-domain simulations, assessing its performance under varying conditions with different nonlinear loads. The proposed PQI is positioned as a valuable tool for monitoring and regulating power quality in distribution systems and residential settings. Its application in the domestic distribution power network is showcased as a means of implementing smart grid technology.

Introduction:

Power quality is characterized by parameters reflecting harmonic pollution, reactive power, and load unbalance. This study examines optimal solutions to these issues and elaborates on their control systems. Field solutions are explained, and corresponding results are presented, demonstrating that employing suitable technology can resolve various power quality issues, making installations trouble-free, more efficient, and compliant with stringent requirements. In contemporary power systems, power quality (PQ) has become a crucial concern for both power providers and consumers. Appropriate PQ solutions are essential at every location where ownership changes hands. Hence, it is crucial to develop a suitable power quality index (PQI) and identify sources and disturbances that degrade PQ. This project focuses on a novel PQI based on the Euclidean norm method. Power quality is directly associated with distortion power generated by nonlinear loads. Enhancing the performance of the previous PQI, it is applied to a practical distribution power system network.

The proposed PQI is constructed as a combination of two factors: the Euclidean norm of total harmonic distortions (THDs) and the electrical load composition rate (LCR) in measured voltage and current waveforms. With the proliferation of electronics, electrical devices have become more sensitive to power quality distortions. While a motor may be somewhat immune to power quality problems, electronic controllers, even as small as a shoebox, efficiently control the performance of a 1000-hp motor.

This project introduces a new distortion power quality index, comprising the LCR estimated by the reduced multivariate polynomial (RMP) model and the Euclidean norm of THDs of measured voltage and current waveforms. The proposed index provides the relative harmonic pollution ranking (HPR) of each nonlinear load in the presence of distorted voltage at the point of common coupling (PCC), ensuring reliable and consistent performance under varying conditions.

Problem formulation:

This project introduces a novel distortion power quality index, incorporating the electrical load composition rate (LCR) estimated by the reduced multivariate polynomial (RMP) model and the Euclidean norm of total harmonic distortions (THDs) in the measured voltage and current waveforms. The aim is to address power quality issues and achieve a reliable and consistent system performance under various conditions. The proposed system offers the relative harmonic pollution ranking (HPR) for each nonlinear load in the presence of distorted voltage at the point of common coupling (PCC). The HPR serves as a practical and significant factor, indicating the extent to which each load affects the PCC through relative rankings in distortion power generation. This project utilizes instrument readings of load currents and voltage at the PCC, eliminating the need for direct calculations of apparent, fundamental active power, and fundamental reactive power.

Implementation of the DPQI^{NEW}

Derivation of the DPQI^{NEW} and LCR estimation

The DPQI^{new} in (2) is now derived from D in (11). Firstly, the term, $(THD_v, THD_i)^2$ in right-hand side of (11) can be ignored because its value is much smaller than the value of $(THD_v^2 + THD_i^2)$. Their rate is defined as the square of multiplication ratio (SMR) in (15).

$$SMR = \frac{THD_v^2 \cdot THD_i^2}{THD_v^2 + THD_i^2} < 0.025 \quad \dots (15)$$

Then, the distortion power D, for the individual nonlinear n load, in Fig. 1 is approximated as follows. Note that $V_{1,PCC}$ and $I_1(n)$ in (16) are fundamental components of each PCC voltage V_{PCC} and loadcurrent I_n , respectively.

$$D(n) \approx V_{1,PCC} \cdot I_n \sqrt{THD(v_{pcc})^2 + THD(i_n)^2} \quad \dots (16)$$

The approximated distortion power in (11) has the same form of Euclidean norm of THDs as the DPQI^{new}. Thereafter, the analysis of the relation between $V_{1,PCC}$, $I_1(n)$ in (11) and $LCR(i_n)$ gives the final solution to derive DPQI^{new} from D. For formulation of the LCR estimation, the relation between the total electric current $i(t)$, and the load currents i_1, i_2, \dots, i_n , is modelled as (17) with their normalized values, which are denoted by the superscript, norm. The normalization is achieved by making each fundamental component of measured current to be unity in its magnitude.

$$i^{norm}(t) = k_1 i_1^{norm}(t) + k_2 i_2^{norm} + \dots + k_n i_n^{norm}(t) \dots (17)$$

where k_1, k_2, \dots, k_n are the unknown coefficients, without any calculation of powers, they provide the actual rate of the composition of each load current with respect to total current. Also, without regard to measurement scales used with different current Transformer (CT) ratios the estimation scheme through the normalization is always valid. This LCR can give a standard for current injection limits from each load with the benefit of being an effective evaluation tool for the effects of individual load types. Each load current $i_n(t)$, is formed by the superposition of all harmonic components including its fundamental, which is higher than the other harmonic components. Then, the LCR is proportional to the rate of its fundamental components; therefore, $V_{1,PCC}$, $I_1(n)$ and $LCR(i_n)$ also have the proportional relationship. Finally, the relative HPR provided by the DPQI^{new} represents the original ranking for the associated of nonlinear loads.

To estimate the LCR the RMP model is applied. This optimization technique is a kind of

training algorithm to search the weight parameters for the nonlinear input/output mapping such as NN. The main advantage of the RMP model over NNs is that it has the on e-shot training property.

The relative HPR provided by the DPQI^{new} represents the original ranking for the associated of nonlinear loads. In other words, it does NOT require iteration procedures during the process to find a solution weight vector. The brief descriptions for the RMP model are summarized in below.

Reduced Multivariate Polynomial Model

The general multivariate polynomial (MP) model can be expressed as:

$$g(\alpha, x) = \sum_i^K \alpha_i x_1^{n_1} x_2^{n_2} \dots x_n^{n_n} \quad \dots (18)$$

where the summation is taken over all nonnegative integers n_1, n_2, \dots, n_n for which $n_1 + n_2 + \dots + n_n \leq r$ with r being the order of approximation. 'x' denotes the regressor vector as $[x_1, \dots, x_n]^T$ containing inputs and the vector $\alpha = [\alpha_1, \dots, \alpha_k]$ is the parameter vector to be estimated. K is the total number of terms in $g(\alpha, x)$.

The general MP model in (18) can be replaced with (19) by using the parameter vector, α and the function(x), which is composed of variables of the regressor vector.

$$g(\alpha, x) = \alpha^T p(x) \quad \dots (19)$$

Given m data points with $m > K$ and using the least-squares error minimization error objective given by

$$g(\alpha, x) = \sum_{i=1}^m [y_i - g(\alpha, x)] + b \| \alpha \|^2$$

$= [y - P\alpha]^T [y - P\alpha] + b\alpha^T \alpha \quad \dots (20)$ where b is a regularization constant and $\| \alpha \|^2$ denotes the Euclidean norm, objective function (15) after minimizing the error result in

$$\alpha = (P^T P + bI)^{-1} P^T y \quad \dots (21)$$

where $P \in R^{m \times K}$ denotes the Jacobian matrix $p(x)$ of , and $y = [y_1, \dots, y_m]^T$, and I is the $K \times K$ identity matrix.

Weierstrass approximation theorem includes that every continuous function defined on an interval can be approximated as closely as desired by a polynomial function. However, the number of independent adjustable parameters would grow as r^r for the r^{th} -order model with input dimension. Thus, the MP model would need a huge quantity of training data to ensure that the parameters are well determined. To significantly reduce the huge number of terms in the MP model, the RMP model is considered,

$$\hat{f}_{RMP}(\alpha, x) = \alpha_0 + \sum_{k=1}^r \sum_{j=1}^l \alpha_{kj} x_j^k + \sum_{j=1}^r \alpha_{rl} + j(x_1 + x_2 + \dots + x_l)^j + \sum_{j=2}^r (\alpha_j^T \cdot x)(x_1 + x_2 + \dots + x_l)^{j-1},$$

... (22)

The number of terms in this model can be expressed as $K=1+r+l(2r-1)$. It is shown that when compared to the MP model, the RMP model, in which the number of weight parameters increases linearly, is a much more efficient algorithm in a complicated polynomial system with the higher-order, in which the number of parameters increases exponentially with respect to the order of polynomials.

The preceding MP regression provides an effective way to describe complex nonlinear input-output relationships. However, for the r th-order model with input dimension l , the number of independent adjustable parameters would grow with Lr . Thus, the MP model would need a huge quantity of training data to ensure that the parameters are well determined. To significantly reduce the huge number of terms in the MP model, the following model in (23) is considered:

$$\hat{i}_{MN}(\alpha, x) = \alpha_0 + \sum_{j=1}^r (\alpha_{j1}x_1 + \alpha_{j2}x_2 + \dots + \alpha_{jl}x_l)^j$$

... (23)

It is noted that this gives rise to a nonlinear estimation model where the weight parameters may not be estimated in a straightforward manner. Although an iterative search can be formulated to obtain some solutions, there is no guarantee that these solutions are global. The following RMP model can be written as

The RMP model is a much more efficient algorithm in a complicated polynomial system with higher order, in which the number of weight parameters linearly increases, compared with the MP model, in which the number of parameters exponentially increases with respect to the order of polynomials.

As mentioned before, it is necessary to compute the values of the LCR and THD for the harmonic load currents to implement the DPQI. The RMP model is now applied to estimate the two aforementioned factors.

Note that the proposed DPQI exploits distortion in the only current waveform without

considering that in voltage for both the LCR and THD. To take into account the case in existence of a distorted voltage, the nonlinear load harmonics are predicted by the same RMP model to calculate the proper THD.

The estimation of nonlinear load harmonics, which as required to implement the DPQI^{old}, is not necessary here for calculating the THD of waveforms. Therefore, it avoids applying another RMP model.

Evaluation of Performance

To evaluate the performance of the RMP model applied to the estimation problems, the RMSE and mean-absolute-percentage error (MAPE) in where y_m and \hat{y}_m are the actual and estimated values, respectively, and n represents the number of data samples, are computed with the measurement of the actual current waveforms.

$$RMSE = \sqrt{\frac{1}{n} \sum_{m=0}^{n-1} (y_m - \hat{y}_m)^2}$$

$$MAPE = \frac{1}{n} \sum_{m=0}^{n-1} \frac{|y_m - \hat{y}_m|}{y_m} \quad \dots(24)$$

The RMSE uses the absolute deviation between the estimated and actual quantities. Due to squaring, the RMSE gives more weight to larger errors than smaller ones. The MAPE is, on the other hand, dimensionless and can thus be used to compare the accuracy of the model on different series.

Simulation Results

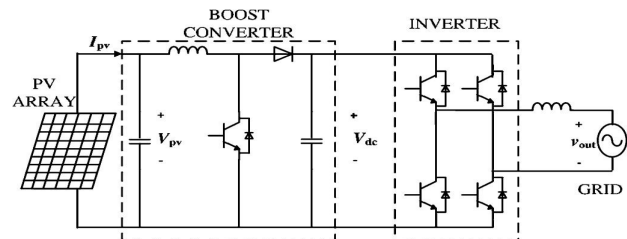


Fig 5.3.1 Schematic circuit of the inverter system.

The single-phase 3 kW photovoltaic (PV) grid-connected inverter systems and its schematic circuit is shown in Fig 5.3.1. It consists of a dc-dc boost converter, a dc-link capacitor, and a dc-ac inverter. The dc-dc boost converter steps up the PV voltage, which has a wide range corresponding to solar irradiance, to the dc-ac inverter outputs the rated voltage of 220 V with 60 Hz. It operates with the maximum power point tracking (MPPT) control, which extracts the maximum possible power from the PV array, and the current control for power factor correction. The output voltage qualified with the THD within 5% according to IEEE standard 1547.

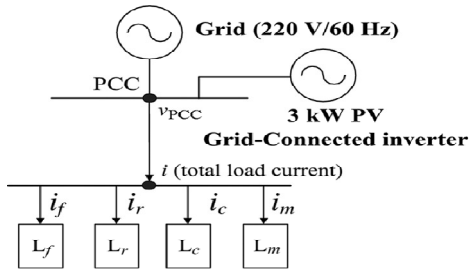


Fig 5.3.2 One-line diagram of proposed system for data acquisition

An acceptable level of the dc-link capacitor voltage V_d , by controlling the gate signal. Fig.5.3.2 shows the one-line diagram of the experimental implementation used to obtain the associated sampling data. The grid-connected inverter system plays the role in distorting the PCC voltage with the low THD within 5%.

Then, the four nonlinear loads are connected to the PCC. These are the fluorescent lighting, radiator, computer, and motor, which are denoted by the subscripts f , r , c , and m , respectively.

The one line diagram explains the point of common coupling of grid connected inverter. The four loads are connected at the point of common coupling. Without losing the generality, the other experimental set-up can be similarly implemented, for example, as a small distribution system extended in power-scale with a 50 kW-scale PV based DG and typical loads such as commercial buildings, factories, and water treatment facilities, etc.

Simulink model for calculating for new power quality index:

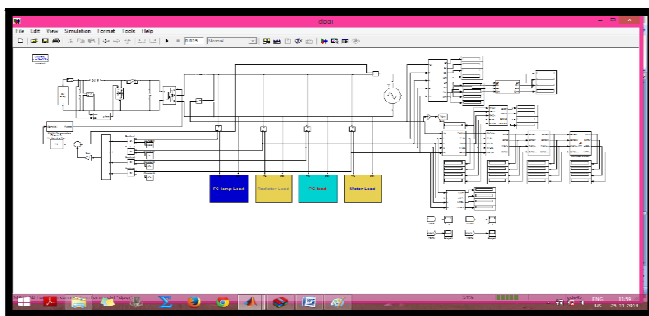


Fig 5.3.3 Proposed DPQI model

The voltage $V_{PCC}(t)$, and the total electric load current $i(t)$, at the PCC in Fig.5.3.4 are measured simultaneously during one period T of the fundamental. It is shown from Fig. 5.3.5 that is lagging and that both are slightly distorted.

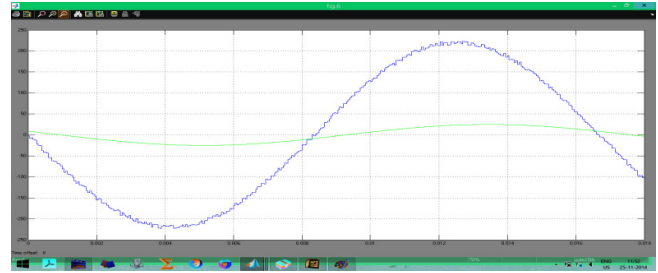


Fig 5.3.4 the voltage $V_{PCC}(t)$, and the total electric load current $i(t)$, at the PCC during one period of the fundamental.

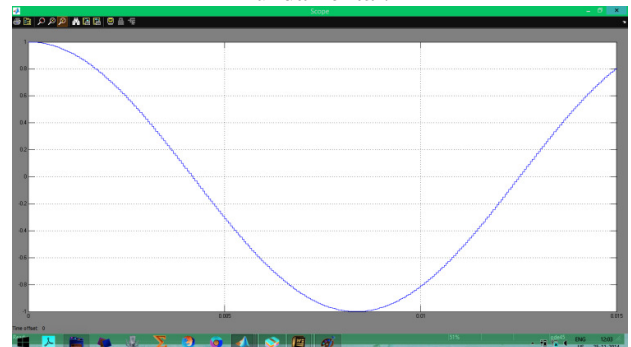


Fig. 5.3.5 Normalized load currents of i_r during one period of the fundamental.

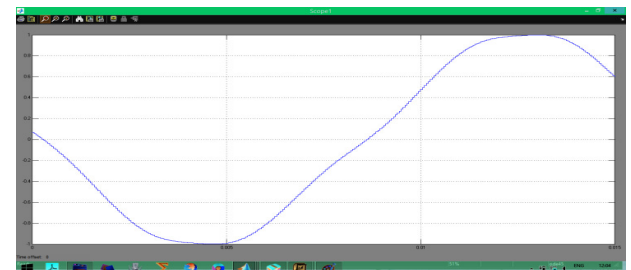


Fig. 5.3.6 Normalized load currents of i_r during one period of the fundamental.

The normalized load current of fluorescent lamp will be as shown above. The data from the above fig 5.3.5 can be used for calculating the Harmonic Pollution Ranking.

The fig.5.3.6 shows the load current wave form for radiator. This curve will be drawn between load current and time.

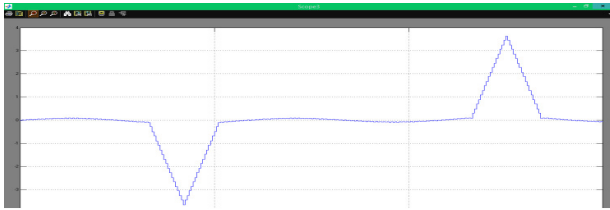


Fig. 5.3.7 Normalized load currents of ic during one period of the fundamental.

The fig 5.3.11 shows the normalized load current of computer for a period of time. This data can be utilised for calculating HPR and LCR.

All load currents i_f , i_r , i_c and i_m are measured, and their normalized waveforms with respect to their own fundamental components are shown in above figures.

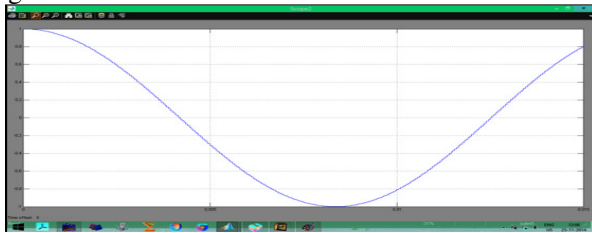


Fig. 5.3.8 Normalized load currents of i_m during one period of the fundamental.

Again, all load currents the degree of their distortion is more severe than $i(t)$ lagging $V_{PCC}(t)$. Each load current waveform (normalized) and the harmonics of $V_{PCC}(t)$ are calculated by using discrete-time-Fourier-transform (DTFT). The sampling frequency of all obtained waveforms is 500,000 Hz in this Fourier analysis, which is high enough to satisfy the Nyquist theorem with respect to the other high-frequency (up to 20th-order) components as well as the fundamental.

Table 5.1 THDs of PCC voltage and load currents

Load type	Fluorescent	Radiator	Computer	Motor
THD(V_{PCC}) [%]	3.78			
THD(i) [%]	11.7	4	145.4	5.33

With the data in above figures THDs of the PCC voltage and load currents are calculated, according to the definition of THD.

It is observed that the PCC voltage is distorted with the small THD of 3.78%, which is reasonably acceptable, from the results in Table 5.1.

All nonlinear loads are affected by the distortion from and therefore have more harmonic currents than those generated due to their own nonlinearity. Also, note that the load current, injected into the computer is most severely distorted with the highest THD of 145.36%.

THDs of PCC voltage and load currents are tabulated. The tabular column gives the total harmonic distortion of voltage and current'

Calculation of the DPQI^{NEW}

It is now ready to calculate the according to the procedure in Fig. 2. Firstly, the sixth-order ($r=6$) RMP model, which provides the best performance after testing several RMP models with the other orders, is applied to find the LCR. Then, its solution vector, L is obtained.

$$L = [k_1, k_2, k_3, k_4]^t = [LCR(i_f), LCR(i_r), LCR(i_c), LCR(i_m)]^t = [0.062, 0.7961, 0.0181, 0.1237]^t$$



Fig. 5.4.1 Estimation of the total current $i(t)$, by the RMP model.

With this LCR, the result of estimating the total load current $i(t)$, is given in Fig. 5.4.1 This shows very good estimation performance. Simulink model for finding total load current is as shown below.

Simulink model for finding total load current:

Fig 5.4.2 Simulink model for finding total load current Also, when it is compared with the actual LCR of apparent powers, LCR (S_a), its performance is shown in Table 5.2.

Table 5.2 LCR of apparent powers and L

Load type	Fluorescent	Radiator	Computer	Motor
S_a [VA]	245	3134	126	487
LCR(S_a)	0.0614	0.7853	0.0315	0.122
L	0.0614	0.7853	0.0315	0.122

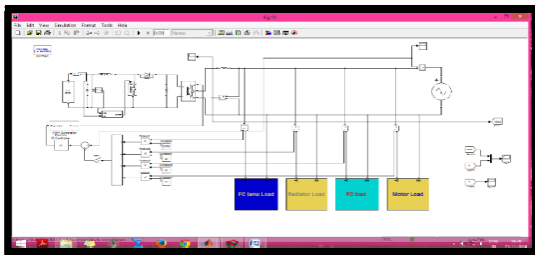
Even though the distortion of computer is severe, the values of LCR (S_a) and L are acceptably matched. Thereafter, the DPQI^{new} in (2) is finally computed with the previously obtained THDs of voltage and current waveforms. Its values are [0.7312, 4.3853, 2.6363, and 0.8090] for the given nonlinear loads, which are fluorescent, radiator, computer, and motor, respectively.

Determination of the HPR

By dividing the DPQI^{NEW} by the sum of its each value, the normalized relative ratio of the index (DPQI_R^{NEW}) is obtained as [0.0854, 0.5122, 0.3079, 0.0945]. Then, the relative HPR is determined by the order of magnitude of the DPQI^{NEW}, and the result is given in Table 5.3.

Table 5.3 DPQI^{NEW} and its corresponding HPR

Load type	Fluorescent	Radiator	Computer	Motor
DPQI ^{new}	0.7312	4.385	2.636	0.809
DPQI _R ^{new}	0.0854	0.5122	0.3079	0.0945
HPR	4	1	2	3
D[VA _d]	29.2	192.5	104.1	33.33



D _R	0.0813	0.5361	0.2899	0.0928
SMR	0.0013	0.0008	0.0014	0.001

Each factor of DPQI_R^{NEW} indicates how much each load takes the portion of distortion power, D generated from each load with respect to the PCC in an overall system. It can be observed from Table III that the ‘radiator’ has the worst effect on the system by aggravating power quality problem with the highest HPR even though its current has the lowest THD among the four load currents.

On the other hand, the distortion power D, for each load is computed by (3) as

$$D = [29.20, 192.54, 104.11, 33.33]$$

Similarly to the calculation of DPQI_R^{NEW}, its normalized relative ratio (D_R) is obtained as [0.0813, 0.5361, 0.2899, 0.0928], and is shown in Table 5.3.

The order in its magnitude is exactly the same as that of. This proves that the HPR represents the exact ranking of the distortion power produced from the nonlinear loads. Also, Table III shows that the values of SMR, which is defined to validate the proposed DPQI^{NEW} for the distortion power, are very small as mentioned earlier.

These experimental results verify that the DPQI^{NEW} can be effectively used as a decision-making index for power quality ranking without requiring the direct measurement of distortion powers of each nonlinear load.

The proposed system is used to make a decision about the power quality index, which means it gives the Harmonic Pollution Ranking to the loads which are distorted.

Drawback of the DPQI^{OLD}

For the same measurement obtained in above, the DPQI^{OLD} in (1) is now calculated. The solution vector L, to estimate the LCR is already given as

$$L = [0.062, 0.7961, 0.0181, 0.1237]^t$$

As mentioned before, the THD (i_n) in (1) is calculated with the estimated (not measured) load currents with the assumption that a pure sinusoidal voltage is supplied to the PCC. Therefore, another RMP model with the eighth-order (r=8) is applied to estimate the exact nonlinear load harmonics.

Except for the i_r (t) injected into the radiator, which has the small phase difference with the V_{PCC} (t). The estimation performances for the other currents are poor. Simulink model for finding DPQI^{OLD} is as shown below

Simulink model for calculating DPQI^{old}:

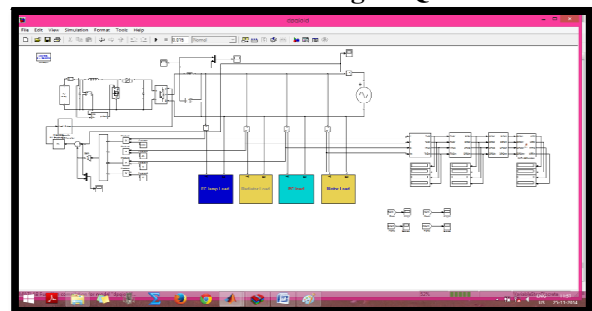


Fig 5.6.1 DPQI^{OLD} model

The results of DPQI^{OLD} and its corresponding HPR are given in Table 5.4.

Table 5.4 DPQI^{old} and its corresponding HPR

Load type	Fluorescent	Radiator	Computer	Motor
THD(i)[%]	12.03	0.97	77.52	21.6
DPQI _R ^{old}	0.7459	0.7716	1.403	2.671
HPR	4	3	2	1

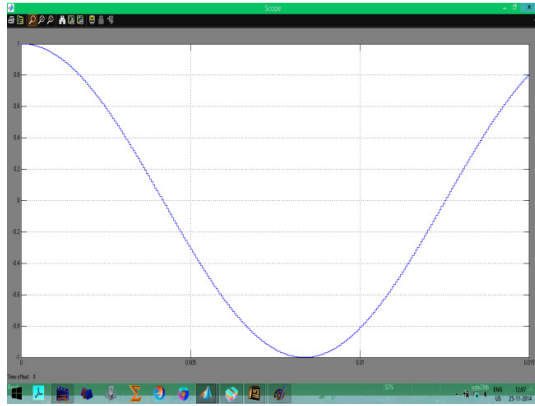


Fig 5.6.2 Estimation of load current i_r by the RMP model

The above figure shows the fluorescent load current by RMP model. It is clearly show that with the incorrect HPR they give totally wrong answers. This proves that when the load current is severely distorted like the $i_c(t)$ the DPQI^{OLD} has the serious drawback and/or with a low power factor it has a large phase difference with the $V_{PCC}(t)$. The figure 5.6.3 shows the radiator current which is normalized. The graph gives the distorted power quality index information.

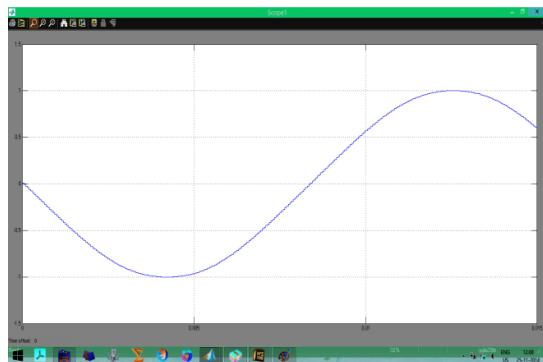


Fig 5.6.3 Estimation of load current i_r by the RMP model



Fig.5.6.4 Estimation of load current i_c by the RMP model

The above figure is for load current that is computer normalized current by the RMP model. This figure is used for calculating HPR. This proves that when the load current is severely distorted like the $i_c(t)$ the DPQI^{OLD} has the serious drawback .

The figure 5.6.5 represents the motor load current which is calculated from RMP model.

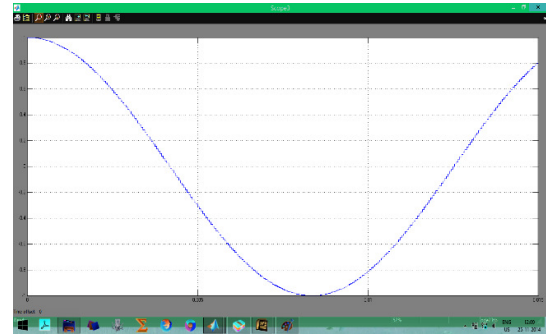


Fig 5.6.5 Estimation of load current i_m by the RMP model

Tests In Three-Phase Balanced System

The clear definition of distortion power is necessary to evaluate and verify the DPQI^{new}. Although many theories have been developed for the single-phase case, their extension to the three-phase system is also important. Therefore, the proposed index is now applied to a three-phase balanced system

It is small enough to prove the good estimation performance of the proposed .Also, the performances of and to determine the HPR are compared in Table 5.4. It is clearly shown that the proposed has the superior performance to the. In Table 5.3, the relationship between and was not perfectly linear even though they are closely related.

Harmonic Current Injection Model

For the harmonic load modelling, several methods such as a constant current source (CCS), crossed frequency admittance matrix (CFAM), Norton model, and harmonic current injection model have been commonly used. These can be selected by considering the trade-off between simplicity and sensitivity. In this project, the harmonic current injection model is properly chosen on the purpose of simulation. In this method, any loads are represented by aggregating each effect of individual loads at a distribution level. Then, the aggregate harmonic load is represented by a harmonic current source in parallel with some linear impedance.

The one-line diagram of system used in the simulation is shown with the representation of harmonic loadsas mentioned before, the grid-connected inverter system plays the role in distorting the PCC voltage with the low THD within 5%

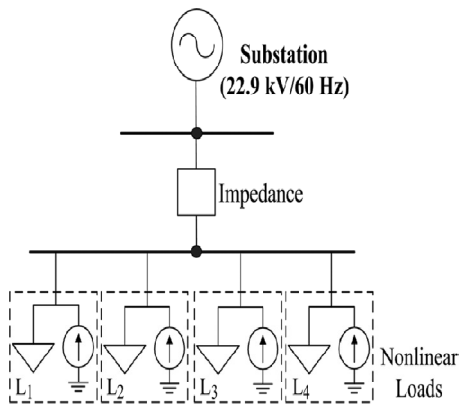


Fig 5.8.1 One-line diagram of system used in the simulation by the harmonic current injection model.

Then, the four nonlinear loads, which are selected by the load classification guide, are connected to the PCC. These are the fluorescent lighting, radiator, computer, and motor, which are denoted by the subscripts f, r, c and m, respectively. For example, as a small distribution system extended in power-scale with a 50 kW-scale PV based DG and typical loads such as, factories and commercial buildings etc.

Conclusion

This project proposed the new distortion power quality index to replace the previously proposed index. Its computation was carried out based on the load composition rate (LCR) and Euclidean norm of total harmonic distortions (THDs) of the measured voltage and current waveforms which are at the point of common coupling (PCC). The model that is reduced multivariate polynomial (RMP) with the one shot training property be successfully applied to estimate the LCR. Moreover, the use of could avoid applying another RMP model, which is required in the implementation of to estimate the nonlinear load harmonics. This advantage allows for more effective and preferable use in practice. Also, the experimental results showed that the can provide the relative harmonic pollution ranking (HPR) of several nonlinear loads with good performance, which is directly related to their distortion powers without the need for direct measurements. In contrast, the results also verified that it has the serious drawback of obtaining wrong answers with an incorrect HPR. This was the case when the load current was severely distorted with the high THD and/or when it had a large phase difference with the PCC voltage with a low power factor.

References

[1] A. Hajizadeh and M. K. Colkar, "Power flow control of grid-connected fuel cell distributed generation system," J. Electr. Eng. Technol., vol.3, no. 2, pp. 143–151, Jun. 2008.

[2] J. Arrillaga, N. R. Watson, M. H. J. Bollen "Power quality following deregulation," Proc. IEEE, vol. 88, no. 2, pp. 246–261, Feb.2000.
 [3] J. Stones and A. Collinson, "Power quality," IEEE Power Eng. J., vol.15, no. 2, pp. 58–64, Apr. 2001.
 [4] M. F. McGranaghan, "Economic evaluation of power quality," IEEE Power Eng. Review, vol. 22, no. 2, pp. 8–12, Feb. 2001.
 [5] IEEE Standard 519-1992, IEEE "Recommended Requirements and practices for Harmonic Control in Electrical Power Systems, Jun. 1992.
 [6] IEEE Standard "Interconnecting Distributed Resources with Electric Power Systems, July. 2003.
 [7] "What is wrong with the Budeanu concept of distortion power and reactive and why it should be abandoned," IEEE Trans. Instrum. Meas., vol. IM-36, no. 3, pp. 834–837, Sep. 1988. L. S. Czarnecki,
 [8] IEEE Standard "Use Standard Definitions for the Measurement of Electric Power Quantities Under Sinusoidal, Balanced, Nonsinusoidal, or Unbalanced Conditions, IEEE Standard 1459-2000, January. 2000.